Korean J. Chem. Eng., 32(12), 2449-2455 (2015)
DOI: 10.1007/s11814-015-0097-8

pISSN: 0256-1115
eISSN: 1975-7220

Effect of *Paecilomyces cateniannulatus* on the adsorption of nickel onto graphene oxide

Xiaoyu Li, Fengbo Li†, and Lejin Fang

The School of Life Science and Environmental Science, Huangshan University, Huangshan 245041, China
(*Received 12 November 2014 • accepted 12 May 2015*)

Abstract−Graphene oxide (GO) was synthesized by chemical oxidation method and used to remove nickel (Ni(II)) from aqueous solutions in the presence of *Paecilomyces cateniannulatus (P. cateniannulatus*). Based on characteristic results, it was demonstrated that *P. cateniannulatus* was easily combined with carboxyl groups of GO by covalent bond. The adsorption results showed that *P. cateniannulatus* facilitated the adsorption of Ni(II) on GO over a wide range of pH. The maximum adsorption capacities of GO+*P. cateniannulatus* and GO calculated from Langmuir model at pH 4.0 and T=303 K were 104.2 and 81.3 $mg \cdot g^{-1}$, respectively. According to the analysis of thermodynamic parameters, the adsorption of Ni(II) on GO+*P. cateniannulatus* was endothermic and spontaneous. The highlight of this study quantitatively assessed the effect of bacteria on the fate and transports of heavy metals in near-surface geologic systems.

Keywords: Graphene Oxide, Nickel, *Paecilomyces cateniannulatus*, Surface Functional Groups

INTRODUCTION

Nickel (Ni(II)), a common heavy metal, is extensively used in batteries, electroplating and coinage [1-3]. The excessive discharge of Ni(II) into the environment can cause various cancers, such as lung and bone. The maximum permissible concentration of Ni(II) in aqueous solution is 0.02 $mg \cdot L^{-1}$ [4]. The removal of Ni(II) by various adsorbents such as clay minerals [6-9], iron (hydr)oxides [10-12], and carbon-based materials [13-16] has been recently investigated by batch techniques. In these studies, the effect of various environmental factors (i.e., pH, initial concentration and ionic strength) on the adsorption of Ni(II) was extensively investigated by batch technique. However, the low adsorption capacity of these natural adsorbents limited the practical application of the removal of Ni(II) from large volumes of aqueous solution.

Graphene oxide (GO) has been extensively employed to remove heavy metals due to the huge specific surface area, massive oxygenated functional groups, and high chemical affinity [17-20]. It has been demonstrated that GO suspension can be dispersed in aqueous solution sufficiently due to the presence of substantial amounts of hydroxyl and epoxy groups on the basal plane and small amounts of carboxyl groups at the sheet edges of GO [21-23]. Romanchuk et al. [20] found that the maximum adsorption capacity of GO at pH 5.0 was 116 and 760 $\mu mol \cdot g^{-1}$ for U(VI) and Eu(III), respectively. However, to the authors' knowledge, the effect of microbes on the adsorption of heavy metals onto GO is not available in recent years.

Paecilomyces cateniannulatus (P. catenlannulatus) is carnivorous fungi specialized in trapping and digesting nematodes, which lives in the nematodes mostly with glue traps or in rings [24,25]. *P. catenlannulatus* has been recently used as a promising adsorbent to remove heavy metals due to a variety of functional groups such as hydroxyl, carboxyl and phosphorous groups [26-30].

The objectives of this study were (1) to synthesize GO by chemical oxidization method and to characterize its morphology by using SEM, optical microphotograph, FTIR and Raman techniques; (2) to investigate the effect of *P. catenlannulatus* on the adsorption of Ni(II) onto GO by using batch techniques; and (3) to elucidate the interaction mechanism between Ni(II) and GO+*P. catenlannulatus*. This study highlights the effect of microbes on removal of heavy metals in near-surface geologic systems.

MATERIALS AND METHOD

1. Synthesis of GO

The GO was synthesized by the oxidation of flake graphite under vigorous stirring conditions [31]. Briefly, 4.0 g flake graphite and 3.0 g $NaNO_3$ (co-solvent) were added into 300 mL concentrated 96% H_2SO_4 under vigorous stirring and ice-water bath conditions; then 9.0 g of $KMnO_4$ was slowly added over about 2 hr. The suspension was continually stirred for five days at T=298±1 K. Then 30 mL H_2O_2 (30 wt%) was added in the suspension, and the mixture was stirred for 2 hr at room temperature. The removal of impurity in the suspension was washed by DI water and then was centrifuged at 23,000 rpm several times until the pH returned to neutral. The aforementioned suspension was dispersed using vigorous stirring and bath ultrasonication for 30 min at the power of 140 W, the GO suspension were obtained by the collection of supernate after centrifugation at 2,300 rpm for 30 min. The centrifugation and ultrasonication were recycled for several times, and then the sample was rinsed with Milli-Q water until the solution was neutral. The few-layered GO powder was obtained by freeze-drying it in a vacuum tank overnight.

2. Preparation of *P. cateniannulatus*

P. cateniannulatus (strain 13, culture collection of microbiology laboratory, University of Huangshan, China) was isolated from in-

†To whom correspondence should be addressed.
E-mail: lfb@hsu.edu.cn, 0550-6732966@163.com

fected pupae of the lipidopteran *T. pityocampa* in NE China. Culture medium was prepared by adding various salts (e.g., 2.0 g KH_2PO_4, 1.0 g NaH_2PO_4, 1.0 g NH_4Cl, 0.2 g $MgSO_4{\cdot}7H_2O$, 0.01 g $FeSO_4{\cdot}7H_2O$) and 10.0 g glucoses into 1 L DI water; then the mixtures were sterilized at 120 °C for 30 min. Induction of proteases was carried out in solid media: Petri dishes with 0.5% gelatin and 1% (w/v) agar in the above salt solution were prepared. Three replicate dishes were inoculated in the center with a 5×5 mm fragment from the edge of a seven-day-old *P. cateniannulatus* colony. Plates were incubated at 25 °C in the dark for 12 days. After inoculation, the diameters of both colony and halo of gelatin degradation were recorded for each plate every the other day. Proteolytic activity was estimated as an index (1-colony diameter/diameter of halo).

Ni(II) stock solution (60 mg/L) was prepared by dissolving Ni $(NO_3)_2$ (99.9% purity, Sinopharm, China) with DI water and then dilution with 0.01 mol/L HNO_3 solution. All chemicals (Sigma-Aldrich) in analytical reagents were employed directly with further purification in this study.

3. Characterization

SEM images were recorded by a JEOL scanning electron microscope equipped with Noran Voyager X-ray energy-dispersive spectroscopy. The optical microphotograph of *P. cateniannulatus* was conducted by binocular biological microscope (XSP-2(2CA, Shanghai Precision and Scientific Instrument Corporation, Shanghai). FTIR measurements were performed by using a Perkin-Elmer 100 Fourier transform infrared spectrometer equipped with attenuated total reflection sensor in pressed KBr pellets. Spectra at 1.4 cm^{-1} resolution were acquired by co-addition of 128 scans within the 400-4,000 cm^{-1} region. The sensor and KBr background spectrum was calibrated before each measurement. Spectral processing including subtraction of gas compensation (CO_2 vapor) and baseline correction were carried out using MAT-LAB 7.4 computing environment. The Raman spectra were recorded at 514.5 nm by the LabRam HR Raman spectrometer with Ar^+ laser. The BET specific surface area, outer surface area and pore size of GO were obtained by using Automated Surface Area and Pore Size Analyzer (Quadrasorb, USA).

4. Batch Adsorption Experiments

The effect of *P. catenlannulatus* on Ni(II) adsorption onto 0.5 g·L^{-1} GO was investigated in polycarbonate tubes covered with alumina foil-lined Teflon screw caps to prevent degradation of microbes during adsorption experiments. An aliquot of GO suspension was added into 0.1 mol·L^{-1} background electrolyte ($NaClO_4$ solution) containing 200 mg·L^{-1} NaN_3 (as bio-inhibitor) to pre-equilibrate it. The diluted Ni(II) solution was titrated into the aforementioned suspension slowly to avoid the formation of precipitates. The pH of suspensions was adjusted by adding negligible volumes of 0.01-1.0 mol·L^{-1} HNO_3 or NaOH solution using a glass combination electrode (pH/conductivity meter, Fisher Scientific). After adsorption equilibrium, the solid phases were separated from liquid phases by centrifuging it at 9,000 rpm for 30 min. Parallel blank experi-

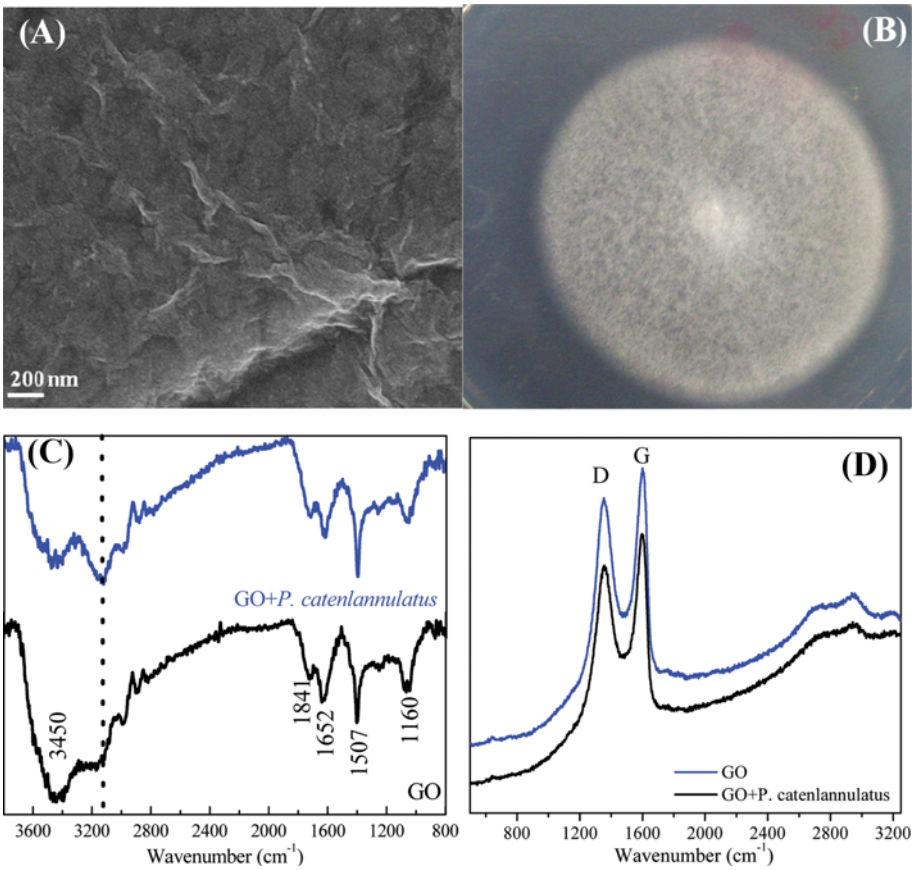

Fig. 1. Characterization of GO and *P. catenlannulatus* used in this study. (A) SEM image of GO; (B) optical microphotograph of *P. catenlannulatus*; (C) FTIR sepectra of GO and GO+*P. catenlannulatus*; (D) raman spectra of GO and GO+*P. catenlannulatus*.

ments were also included in each set of adsorption experiments. The concentrations of Ni(II) were analyzed directly by atomic adsorption spectroscopy (AAS-6300, Shimadzu, Japan). The adsorbed Ni(II) concentrations were estimated by the difference between initial concentration references and the corresponding equilibrium liquid-phase concentrations. All experimental data were the average of triplicate determinations and the relative errors were controlled within ±5%.

RESULTS AND DISCUSSION

1. Characterization

The morphologies of GO and *P. catenlannulatus* are illustrated in Fig. 1. As shown in Fig. 1(A), multilayer wrinkled GO was overlaid with random orientations. From Fig. 1(B) *P. catenlannulatus* was ~100×50 nm, as observed in terms of optical micrograph, which was consistent with the previous study [25]. The changes in the surface functional groups of GO and GO+*P. catenlannulatus* were also investigated by FTIR spectra (Fig. 1(C)). The broad peaks of GO at ~1,160, 1,507, 1,652, 1,842 and 3,450 cm^{-1} were assigned to the stretching vibration of epoxy, C=C, carboxyl, carbonyl and hydroxyl, respectively [32,33]. However, the presence of *P. cateniannulatus* resulted in the shift of oxygenated functional groups toward the high wavenumbers, indicating the *P. cateniannulatus* was easily combined with oxygenated functional groups such as hydroxyl and/or carboxyl groups. Note that the carbonyl group of GO+*P. cateniannulatus* was not observed, which could be attributed to the formation of complexes between *P. cateniannulatus* and carbonyl group of GO. According to the Raman spectra (Fig. 1(D)), the D band (~1,350 cm^{-1}) and G and (~1,580 cm^{-1}) were associated with the disordered sp^3-hybridized carbon and graphitic sp^2 carbon atoms, respectively [34]. The D band came from the structural imperfections created by the attachment of oxygenated functional groups on the carbon basal planes [35,36]. For GO+*P. cateniannulatus*, the decrease of relative intensity of D band could be resultinig from the interaction of oxygenated functional groups of GO with *P. cateniannulatus*. The characteristic results indicated that the presence of *P. cateniannulatus* changed the nanostructure and chemical properties of GO. The BET specific surface area of GO was measured 185.6 m^2/g, whereas the outer surface area was 132.4 m^2/g by using t-Plot model [37]. According to Barrett-Joyner-Halenda model, the distribution of pore size at less than 2.0 nm accounted for approximately 25% (Table 1).

2. Adsorption Kinetics

Fig. 2 shows the adsorption kinetics of Ni(II) on GO and GO+*P. cateniannulatus*. The adsorption rates of Ni(II) sharply increased during the initial 3 hr, then increased slowly to reach equilibrium at 12 h, which was consistent with previous study on the adsorption of Ni(II) on oxidized multiwall carbon nanotubes [16]. The initially rapid adsorption may be attributed to the relatively larger available sites on the adsorbent. Approximately 78% and 85% of Ni(II) were adsorbed on GO and GO+*P. cateniannulatus* at 24 h, respectively. The pseudo-first-order and pseudo-second-order kinetic equations were applied to describe the experimental data. Their linear forms are given in Eqs. (1) [38] and (2) [39], respectively:

$$\ln(q_e - q_t) = \ln q_e - k_f \times t \quad (1)$$

$$t/q_t = 1/(k_s \times q_e) + t/q_e \quad (2)$$

where q_e ($mg \cdot g^{-1}$) and q_t ($mg \cdot g^{-1}$) are the amount of Ni(II) adsorbed at equilibrium and at time t, respectively. k_f (h^{-1}) and k_s ($g \cdot (mg \cdot h)^{-1}$) are the pseudo-first order and pseudo-second order kinetic rate constant, respectively. The corresponding kinetic parameters are shown in Table 2. As shown in Fig. 2 and Table 2, the adsorption of Ni(II) on GO and GO+*P. cateniannulatus* systems can be satis-

Table 1. Specific surface area, pore size and content of oxygenated functional group of GO

Specific surface area (BET)	185.6 m^2/g
Out surface area (t-Plot)	132.4 m^2/g
Pore size (<2.0 nm)	24.5%
-OH group content	10.45 wt%
-O- group content	3.63 wt%
-C=O group content	8.64 wt%
-COOH group content	0.53 wt%

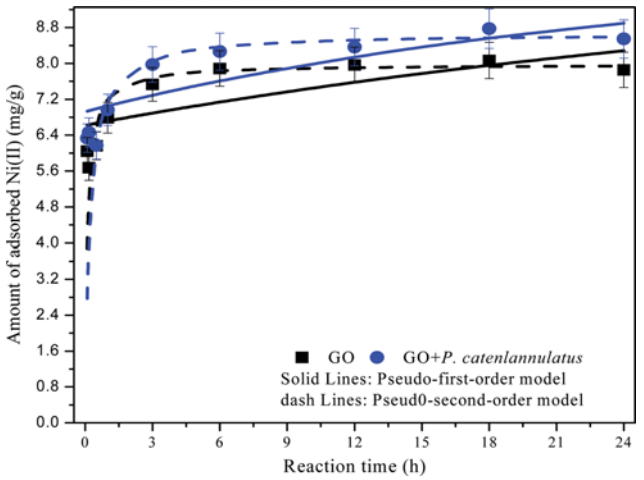

Fig. 2. The adsorption kinetics of Ni(II) on GO and GO+*P. catenlannulatus*, pH 4.0, T=303 K, I=0.1 mol·L^{-1} $NaClO_4$, m/v=0.5 g·L^{-1}.

Table 2. Kinetic constants for the adsorption of Ni(II) onto GO (1) and GO+*P. catenlannulatus* (2)

Adsorbent	Pseudo-first-order			Pseudo-second-order		
	q_e ($mg \cdot g^{-1}$)	k_f (h^{-1})	R^2	q_e ($mg \cdot g^{-1}$)	K_s ($g \cdot (mg\ h)^{-1}$)	R^2
(1)	3.076	0.0428	0.599	7.968	11.409	0.9997
(2)	3.380	0.0282	0.7367	8.658	5.662	0.9995

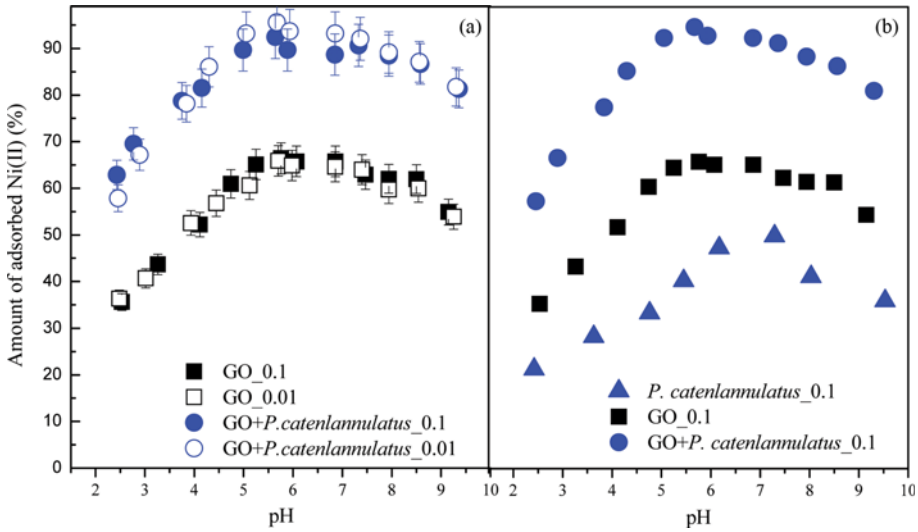

Fig. 3. The adsorption of Ni(II) on GO (a) and GO+*P. catenlannulatus* (b) at different pH and under various ionic strength, T=303 K, m/v= 0.5 g·L^{-1}.

factorily fitted by pseudo-second-order kinetic equation (R^2 >0.999), which indicates that the rate-limiting step of Ni(II) on GO and GO+*P. cateniannulatus* was chemisorption [40].

3. Effect of pH and Ionic Strength

The effect of pH on the adsorption of Ni(II) on GO and GO+*P. cateniannulatus* is shown in Fig. 3. As shown in Fig. 3(a) and (b), the adsorption of Ni(II) on GO, *P. cateniannulatus* and GO+*P. cateniannulatus* increased with increasing pH from 2.5 to 5.5, then maintained this high level at pH 6.0-7.0. Decreased adsorption was observed at pH>7.5, which can be interpreted by the electrostatic interaction. It demonstrated that the pH_{PZC} (pH at point of zero charge) of GO was ~3.84 [18]; therefore, the deprotonation of GO predominately occurred at pH>4.0. The enhanced adsorption of Ni(II) at pH 2.0-5.0 could be attributed to the electrostatic attraction between negatively charged GO and positive charged Ni(II) cations. As shown in Fig. 3(b), the adsorption capacity increased in the order *P. cateniannulatus*>GO>GO+*P. cateniannulatus* significantly. As summarized in Table 1, the content of -OH, -O-, -C=O, -COOH groups was calculated as 10.45, 3.65, 8.64 and 0.53 wt%, respectively. Therefore, a variety of oxygenated functional groups were responsible for the high adsorption of Ni(II) on GO [41]. It was determined that GO was highly negatively charged throughout a wide range of pH 2.0-12.0 [42,43], Therefore, these oxygenated functional groups (e.g., -OH and -COOH) were deprotonated at pH>2.0, which was further proven by the low value of pH_{PZC} (pH at point of zero charge). The negatively charged Ni(II) species were observed at pH>7.5 [44], which probably explained the suppressed adsorption at pH>7.5 due to the electrostatic repul-

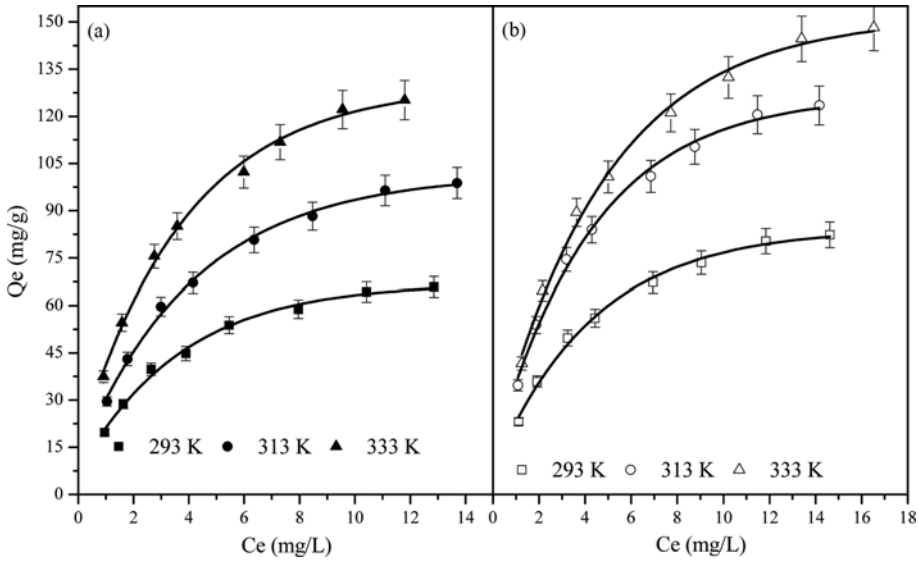

Fig. 4. The adsorption isotherms of Ni(II) on GO (a) and GO+*P. catenlannulatus* (b), pH 4.0, I=0.1 mol·L^{-1} $NaClO_4$, m/v=0.5 g·L^{-1}.

sion between negatively Ni(II) species and negative charged GO. Note that the presence of *P. cateniannulatus* facilitated the adsorption of Ni(II) on GO due to the abundant oxygenated functional groups of *P. cateniannulatus* (Fig. 3(b)). Li et al. demonstrated that *P. cateniannulatus* presented the abundant oxygen-, phosphoryl- and nitrogen-containing functional groups of *P. cateniannulatus* [24,25].

The effect of ionic strength on Ni(II) adsorption on GO and GO+*P. cateniannulatus* is also shown in Fig. 3. The increase of ionic strength had little effect on the adsorption of Ni(II) on GO and GO+*P. cateniannulatus* throughout a wide range of pH, which indicated that inner-sphere surface complexation dominated Ni(II) adsorption on GO. It was determined that the inner-sphere surface complexes were formed by the complexation of adsorbate with amphoteric groups by chemical bonds, which was less ionic strength-dependent [45]. A variety of functional groups of *P. cateniannulatus* contributed to the inner-sphere adsorption of Ni(II) and GO by chemical bonding [46].

4. Adsorption Isotherms

Adsorption isotherms of Ni(II) on GO and GO+*P. cateniannulatus* were investigated at pH 4.0 under different temperature. As shown in Fig. 4(a) and (b), the adsorption of Ni(II) on GO and GO+*P. cateniannulatus* increased with increasing solution concentration. The adsorption of Ni(II) on GO+*P. cateniannulatus* was higher than GO, indicating *P. cateniannulatus* facilitated the adsorption of Ni(II) on GO at low pH conditions. The adsorption isotherms were fitted by Langmuir and Freundlich models; their linear formations can be given in Eqs. (3) and (4), respectively:

$$C_e/Q_e = 1/(b \times Q_{max}) + C_e/Q_{max} \quad (3)$$

$$\log Q_e = \log K_F + 1/n \log C_e \quad (4)$$

where C_e ($mg \cdot L^{-1}$) and Q_e ($mg \cdot g^{-1}$) are the equilibrated concentration of Ni(II) in aqueous solutions and in the adsorbate, respectively. Q_{max} ($mg \cdot g^{-1}$) is the maximum adsorption capacity of adsorbent at complete monolayer coverage. b ($L \cdot mg^{-1}$) and K_F ($mg^{1-n}L^n \cdot g^{-1}$) represents the Langmuir and Freundlich equilibrium constant, respectively. 1/n is the heterogeneity of the adsorption sites.

The corresponding parameters of Langmuir and Freundlich models are tabulated in Table 3. The fitted results revealed that the adsorption of Ni(II) on GO and GO+*P. cateniannulatus* can be well described by Langmuir model (R^2>0.998), which indicated that Ni(II) adsorption on GO and GO+*P. cateniannulatus* was both monolayer adsorption. The maximum adsorption capacities of GO+*P. cateniannulatus* and GO calculated from Langmuir model at pH 4.0 and T=303 K were 104.2 and 81.3 $mg \cdot g^{-1}$, respectively.

5. Thermodynamic Parameters

The effect of temperature on Ni(II) adsorption on GO and GO+*P. cateniannulatus* is also shown in Fig. 4. One can see that the adsorption of Ni(II) increased with increasing temperature from 303 to 333 K, suggesting that Ni(II) adsorption on GO and GO+*P. cateniannulatus* was promoted at higher temperature. Thermodynamic parameters were calculated based on the equilibrium data of isotherms at three different temperatures. The Gibbs free energy change (ΔG^0, $kJ \cdot mol^{-1}$) of the adsorption process can be expressed by Eq. (5):

$$\Delta G^0 = -RT \ln K^0 \quad (5)$$

where R and T are universal gas constant ($8.314\ J \cdot (mol \cdot K)^{-1}$) and Kelvin temperature, respectively. As shown in Fig. 5(a) and (b), the adsorption equilibrium constant ($\ln K^0$) can be calculated by plotting $\ln K_d$ versus C_e and then extrapolating C_e to zero. The adsorption coefficient (K_d) can be calculated by Eq. (6):

$$K_d = (C_0 - C_e)/(C_e * m/v) \quad (6)$$

where C_0 ($mg \cdot L^{-1}$) is the initial Ni(II) concentration, m and v are the mass of adsorbent and volume in this systems, respectively.

The change in entropy (ΔS^0, $kJ \cdot (mol\ K)^{-1}$) and the enthalpy of adsorption (ΔH^0, $kJ \cdot mol^{-1}$) at temperature T (K) can be calculated from the Eq. (7):

$$\Delta G^0 = \Delta H^0 - T\Delta S^0 \quad (7)$$

Based on Eqs. (5)-(7), one can write

$$\ln K^0 = \Delta S^0/R - \Delta H^0/RT \quad (8)$$

As shown in Fig. 5(c) and (d), the values of ΔH^0 and ΔS^0 can be calculated from the slope and intercept of plot of $\ln K^0$ versus 1/T, respectively.

The corresponding parameters are summarized in Table 4. As shown in Table 4, the negative values of ΔG^0 (−25.08 and −24.98 $kJ \cdot mol^{-1}$ at 303 K for GO and GO+*P. cateniannulatus*, respectively) demonstrated that the adsorption of Ni(II) on GO and GO+*P. cateniannulatus* was spontaneous. The value of ΔG^0 of Ni(II) on GO+*P. cateniannulatus* was lower than that of GO, suggesting that Ni(II) was more prone to be adsorbed on GO+*P. cateniannulatus*. The positive values of ΔH^0 (11.93 and 18.47 $kJ \cdot mol^{-1}$ for GO and GO+*P. cateniannulatus*, respectively) indicated that the adsorption of Ni(II) on GO and GO+*P. cateniannulatus* was endothermic, which was consistent with the increased adsorption capacities as the increas-

Table 3. Equilibrium parameters for the adsorption of Ni(II) onto GO(1) and GO+*P. catenlannulatus* (2) at 303, 313, and 333 K

Sample		Langmuir equation			Freundlich equation		
		Q_{max} ($mg \cdot g^{-1}$)	b ($L \cdot mg^{-1}$)	R^2	$\ln k_F$ ($mg^{1-n}L^n \cdot g^{-1}$)	1/n	R^2
(1)	303	104.17	0.267	0.9991	3.232	0.4797	0.96
	313	156.25	0.244	0.9992	3.648	0.481	0.9613
	323	188.68	0.2385	0.999	3.765	0.4786	0.9588
(2)	303	81.30	0.339	0.9987	3.128	0.4554	0.970
	313	123.46	0.301	0.9993	3.4837	0.4619	0.9677
	323	158.73	0.325	0.9989	3.7691	0.4676	0.9729

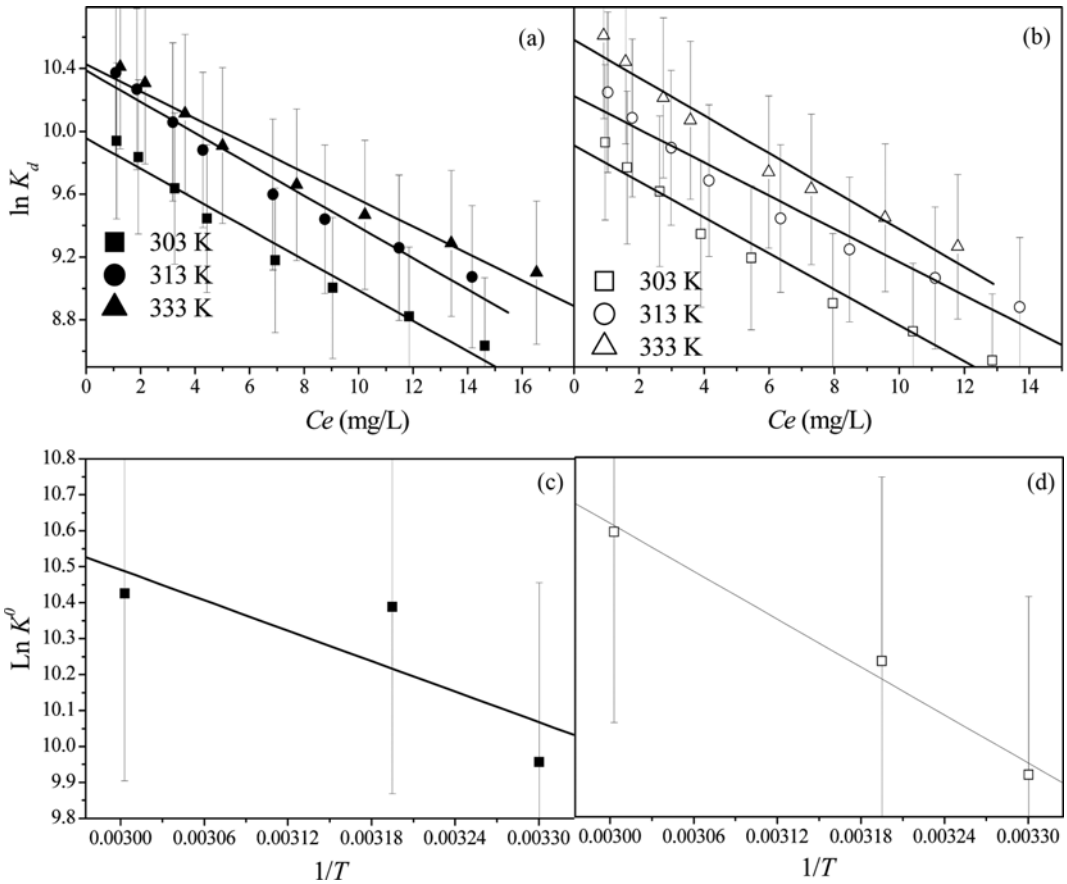

Fig. 5. A and B: Linear plots of log K_d vs C_e of GO (a) and GO+*P. catenlannulatus* (b); C and D: Linear plots of ln K^0 vs 1/T of GO (c) and GO+*P. catenlannulatus* (d), pH 4.0, I=0.1 mol·L^{-1} $NaClO_4$, m/v=0.5 g·L^{-1}.

Table 4. Thermodynamic parameters of Ni(II) adsorption on onto GO(1) and GO+*P. catenlannulatus* (2) at 303, 313, and 333 K

Samples		ΔG^0 kJ·mol^{-1}	ΔH^0 kJ·mol^{-1}	ΔS^0 J·(mol·K)$^{-1}$
(1)	303 K	−25.08	11.73	122.41
	313 K	−26.17		
	333 K	−28.86		
(2)	303 K	−24.98	18.47	143.67
	313 K	−25.78		
	333 K	−29.32		

ing temperature. The positive values of ΔS^0 (122.41 and 143.67 J·(mol· K)$^{-1}$ for GO and GO+*P. cateniannulatus*, respectively) revealed the increased randomness at the solid-liquid interface. The entropy was generally regarded as a measure of the width of the saddle point of the potential energy surface over which reactant molecules must pass as activated complexes. The larger positive entropy of GO+*P. cateniannulatus* revealed dissociative mechanism (ΔS^0>−10 J·(mol·K)$^{-1}$)) [47]. Thermodynamic parameters calculated from temperature-dependent adsorption isotherms suggest that Ni(II) adsorption on GO and GO+*P. cateniannulatus* was endothermic and spontaneous.

CONCLUSIONS

The GO was satisfactorily synthesized by the modified Hummers method and characterized by batch characteristic techniques. The characteristic results indicated that *P. cateniannulatus* was easily combined with oxygenated functional groups of GO. It is determined that the GO can be proposed as one of the excellent adsorbents for the removal of heavy metals in environmental contaminant cleanup. The presence of microbes significantly influenced the fate and transportation of heavy metals from aqueous solution.

ACKNOWLEDGEMENTS

Financial support from 2012 annual national forestry public welfare industry research projects (No. 201304407) is acknowledged.

REFERENCES

1. L. Jarup, Br. *Med. Bull.*, **68**, 167 (2003).
2. K. S. Kasprzak, F. W. Sunderman and K. Salnikow, *Mol. Mech. Mutagenesis*, **533**, 67 (2003).
3. C. Liden and S. Carter, *Contact Dermatitis*, **44**, 160 (2001).
4. K. A. Krishnan, K. G. Sreejalekshmi and R. S. Baiju, *Bioresour. Technol.*, **102**, 10239 (2011).

5. Y. B. Sun, J. X. Li and X. K. Wang, *Geochim. Cosmochim. Acta*, **140**, 621 (2014).
6. Y. Hannachi, N. A. Shapovalov and A. Hannachi, *Korean J. Chem. Eng.*, **27**, 152 (2010).
7. S. S. Gupta and K. G. Bhattacharyya, *J. Colloid Interface Sci.*, **295**, 21 (2006).
8. X. Y. Gu and L. J. Evans, *J. Colloid Interface Sci.*, **307**, 317 (2007).
9. X. Y. Gu, L. J. Evans and S. J. Barabash, *Geochim. Cosmochim. Acta*, **74**, 5718 (2010).
10. J. H. Jeon, B. A. Dempsey, W. D. Burgos, R. A. Royer and E. E. Roden, *Water Res.*, **38**, 2499 (2004).
11. S. Mustafa, M. Irshad, M. Waseem, K. H. Shah, U. Rashid and W. Rehman, *Korean J. Chem. Eng.*, **30**, 2235 (2013).
12. Y. Xu, L. Axe, T. Boonfueng, T. A. Tyson, P. Trivedi and K. Pandya, *J. Colloid Interface Sci.*, **314**, 10 (2007).
13. K. Kadirvelu, K. Thamaraiselvi and C. Namasivayam, *Sep. Purif. Technol.*, **24**, 497 (2001).
14. H. Hasar, *J. Hazard. Mater.*, **97**, 49 (2003).
15. C. Lu and C. Liu, *J. Chem. Technol. Biotechnol.*, **81**, 1932 (2006).
16. C. Jeon, J. Y. Park and Y. J. Yoo, *Korean J. Chem. Eng.*, **18**, 955 (2001).
17. G. X. Zhao, J. X. Li, X. M. Ren, C. L. Chen and X. K. Wang, *Environ. Sci. Technol.*, **45**, 10454 (2011).
18. Y. B. Sun, S. B. Yang, G. X. Zhao, Q. Wang and X. K. Wang, *Chem. Asian J.*, **8**, 2755 (2013).
19. Y. B. Sun, D. D. Shao, C. L. Chen, S. B. Yang and X. K. Wang, *Environ. Sci. Technol.*, **47**, 9904 (2013).
20. W. Jia and S. Lu, *Korean J. Chem. Eng.*, **31**, 1265 (2014).
21. X. Li, G. Zhang, X. Bai, X. Sun, X. Wang, E. Wang and H. Dai, *Nat. Nanotechnol.*, **3**, 538 (2008).
22. F. Kim, L. J. Cote and J. X. Huang, *Adv. Mater.*, **22**, 1954 (2010).
23. Y. B. Sun, S. B. Yang, C. C. Ding, W. C. Cheng and Z. X. Jin, *RSC Adv.*, **5**, 24886 (2015).
24. F. B. Li, Z. M. Gao, X. Y. Li and L. J. Fang, *J. Radioanal. Nucl. Chem.*, **299**, 1281 (2014).
25. F. B. Li, Z. M. Gao, X. Y. Li and L. J. Fang, *J. Environ. Radioact.*, **137**, 31 (2014).
26. L. Zucconi, C. Ripa, F. Alianiello, A. Benedetti and S. Onofri, *Biol. Fretil. Soil*, **37**, 17 (2003).
27. K. Paraszkiewicz, A. Frycie, M. Slaba and J. Dlugonski, *Biomet.*, **20**, 797 (2007).
28. S. S. Ahluwalia and D. Goyal, *Eng. Life Sci.*, **10**, 480 (2010).
29. S. Sharma and A. Adholeya, *Int. Biodeterior. Biodegrad.*, **65**, 309 (2011).
30. J. F. Cardenas-Gonzalez and I. Acost-Rodriguez, *Prog. Biomass. Bioenerg. Prod.*, **27**, 133 (2011).
31. W. S. Hummers and R. E. Offeman, *J. Am. Chem. Soc.*, **80**, 1339 (1958).
32. Z. X. Jin, X. X. Wang, Y. B. Sun, Y. J. Ai and X. K. Wang, *Environ. Sci. Technol.*, **49**, 9168 (2015).
33. D. A. Dikin, S. Stankovich, E. J. Zimney, R. D. Piner, G. H. B. Dommett, G. Evmenenko, S. T. Nguyen and R. S. Ruoff, *Nature*, **448**, 457 (2007).
34. M. A. Pimenta, G. Dresselhaus, M. S. Dresselhaus, L. G. Cancado, A. Jorio and R. Saito, *Phys. Chem. Chem. Phys.*, **9**, 1276 (2007).
35. D. Yang, A. Velamakanni, G. Bozoklu, S. Park, M. Stoller, R. D. Piner, S. Stankovich, I. Jung, D. A. Field, C. A. Ventrice and R. S. Ruoff, *Carbon*, **47**, 145 (2009).
36. Y. B. Sun, S. B. Yang, C. Chen, C. C. Ding, W. C. Cheng and X. K. Wang, *Environ. Sci. Technol.*, **49**, 4255 (2015).
37. J. H. De Boer, B. G. Linsen and T. J. Osinga, *J. Catal.*, **4**, 643 (1965).
38. S. Lagergren, *Handlingar*, **24**, 1 (1898).
39. Y. S. Ho and G. Mckay, *Process Biochem.*, **343**, 451 (1999).
40. W. C. Cheng, C. C. Ding, Y. B. Sun and X. K. Wang, *Chem. Eng. J.*, **269**, 1 (2015).
41. Y. B. Sun, Q. Wang, C. L. Chen, X. L. Tan and X. K. Wang, *Environ. Sci. Technol.*, **46**, 6020 (2012).
42. I. Chowdhury, M. C. Duch, N. D. Mansukhani, M. C. Hersam and D. Bouchard, *Environ. Sci. Technol.*, **47**, 6288 (2013).
43. J. Y. Huang, Z. W. Wu, L. W. Chen and Y. B. Sun, *J. Mol. Liq.*, **209**, 753 (2015).
44. E. Tertre, G. Berger, S. Castet, M. Loubet and E. Giffaut, *Geochim. Cosmochim. Acta*, **69**, 4937 (2005).
45. Y. B. Sun, C. C. Ding, W. C. Cheng and X. K. Wang, *J. Hazard. Mater.*, **280**, 399 (2014).
46. V. A. Sinitsyn, S. U. Aja, D. A. Kulik and S. A. Wood, *Geochim. Cosmochim. Acta*, **64**, 185 (2000).
47. B. A. Fil, R. Boncukcuoglu, A. E. Yilmaz and A. Bayar, *Korean J. Chem. Eng.*, **29**, 1232 (2012).